

How Important are Temperature Effects for Cluster Polarizabilities?

Gabriel U. Gamboa, Patrizia Calaminici,* Gerald Geudtner, and Andreas M. Köster*

Departamento de Química, CINVESTAV, Avenida Instituto Politécnico Nacional 2508,
A.P. 14-740 México D.F. 07000, Mexico

Received: September 10, 2008; Revised Manuscript Received: October 20, 2008

State-of-the-art first-principle all-electron density functional theory calculations on small sodium clusters are performed to study the temperature dependency of their polarizabilities. For this purpose Born–Oppenheimer molecular dynamics simulations with more than 100 000 time steps (> 200 ps) are recorded employing gradient corrected functionals in combination with a double- ζ valence polarization basis set. For each cluster 18 trajectories between 50 and 900 K are collected. The cluster polarizabilities are then calculated along these trajectories employing a triple- ζ valence polarization basis set augmented with field-induced polarization functions. The analysis of these calculations shows that the temperature dependency of the sodium cluster polarizabilities varies strongly with cluster size. For several clusters characteristic changes in the polarizability per atom as a function of temperature are observed. It is shown that the inclusion of finite temperature effects resolves the long-standing mismatch between calculated and measured sodium cluster polarizabilities.

For many years static polarizability measurements have been used to gain insight into the electronic structure of small clusters.¹ Because the polarizability is very sensitive to the distribution of the valence electron density it can also be used as an indicator for chemical reactivity.² Therefore, the study of the size dependency of the polarizability of simple clusters yields results of fundamental importance to chemistry and physics. Particular examples are the polarizability studies on sodium clusters which were of paramount importance for the derivation of the so-called jellium model.³ Today, this model is used with great success in cluster science.⁴ Several reliable experimental data series of sodium cluster polarizabilities are nowadays available in the literature.⁵ In the pioneering work of Knight et al.^{5b} the static polarizabilities of sodium clusters in a size range from 2 to 40 sodium atoms were studied. Later on Rayane et al.^{5c} repeated these measurements for a smaller size range from 2 to 22 sodium atoms. Most recently, Tikhonov et al.^{5d} measured the polarizability of selected sodium clusters up to 93 atoms. The overall agreement between these different experiments is quite satisfying. Nevertheless, discrepancies exist. In particular, the pronounced oscillating behavior observed by Knight et al. up to the hexamer (Figure 1a, circles) was not confirmed by the more recent study of Rayane and co-workers (Figure 1a, squares). To emphasize the spread between these two experimental data sets we have connected the data points in Figure 1 by lines. This figure also shows that for the larger sodium clusters with 7, 8, and 9 atoms excellent agreement between the reported data sets exist. The heptamer and octamer polarizabilities were also measured by Tikhonov et al.^{5d} and are in good agreement with the depicted experimental data in Figure 1, too. To resolve the discrepancy in the measured polarizabilities of the smaller sodium clusters many theoretical studies have been performed over the last two decades (see refs 1a and 6

and references therein). Most calculations employed density functional theory methods⁷ but wave function based studies are also available.^{6a} A comparison of these theoretical studies reveals that the static polarizabilities of sodium clusters are severely underestimated at all reliable levels of theory. For comparison, we depict in Figure 1a the calculated polarizabilities with the theoretical methods employed in this work, too. These calculations are performed with the linear combination of Gaussian-type orbital density functional theory (LCGTO-DFT) deMon2k⁸ code. The crosses refer to all-electron polarizabilities calculated with the local density approximation (LDA) employing the exchange functional from Dirac⁹ in combination with the correlation functional proposed by Vosko, Wilk, and Nusair¹⁰ (VWN). The stars denote polarizabilities obtained with the gradient corrected exchange-correlation functional proposed by Perdew, Burke, and Ernzerhof¹¹ (PBE). The cluster structures were optimized at the corresponding level of theory employing a double- ζ valence polarization (DZVP) basis set.¹² For the polarizability calculations a triple- ζ valence polarization (TZVP) basis set augmented with field induced polarization (FIP) function was used.¹³ All calculations are performed in the framework of auxiliary density functional theory¹⁴ (ADFT) with A2 or GEN-A2* auxiliary function sets. The latter was used in the analytical calculation of the cluster polarizabilities. It is well established in the literature that calculated DFT polarizabilities at this level of theory differ by no more than 5% from experiment. Figure 1a, however, shows that the calculated polarizabilities are not only considerably too low but that even at the level of the gradient corrected PBE functional differences of more than 10% to the experimental values can occur. By and large these results are confirmed by many other theoretical calculations. Over the last two decades different corrections have been proposed to resolve this long-standing discrepancy between theory and experiment, but until now the situation remained unsolved. More recently, it has been speculated that the

* Corresponding author. E-mail: pcalamin@cinvestav.mx and akoster@cinvestav.mx.

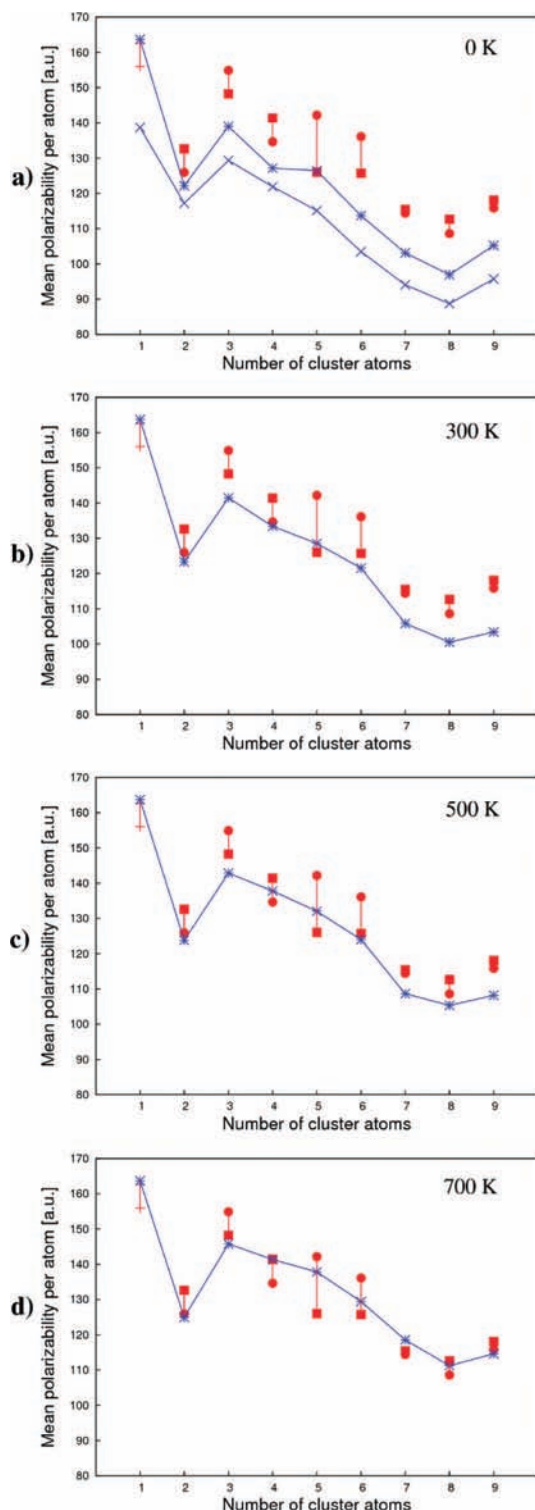


Figure 1. Experimental (atom, Molof et al.;^{7,8} circle, Knight et al.;⁹ square, Rayane et al.¹⁰) and theoretical mean polarizabilities per atom [au] of Na_n ($n = 2-9$) clusters. The theoretical values are calculated at the VWN/TZVP-FIP/GEN-A2* (crosses) and PBE/TZVP-FIP/GEN-A2* (stars) level of theory. These values are connected to guide the eye. The individual graphs display calculated polarizabilities at 0 (a), 300 (b), 500 (c), and 700 K (d). The cluster temperature in the experiment is estimated to be between 400 and 800 K.

mismatch between calculated and measured sodium cluster polarizabilities is due to finite temperature effects.^{6b-d} In fact, this idea was already mentioned in the original experimental work.^{5b} However, a systematic study of the temperature dependency of sodium cluster polarizabilities at a reliable first-

principle all-electron level of theory has, so far, never been performed. In this work we address this question. Therefore, to study the dynamics of small sodium clusters at finite temperatures Born–Oppenheimer molecular dynamics (BOMD) calculations are performed at the above-described PBE/DZVP/A2 level of theory. For each cluster, from the dimer to the nonamer, 18 trajectories are recorded in a temperature range from 50 to 900 K with intervals of 50 K. Each trajectory has a length of 220 ps and was recorded with a time step of 2 fs. Similar statistics already have been successfully applied to determine the melting temperatures of sodium clusters with LDA pseudo-potential DFT molecular dynamics. The temperature in the canonical BOMD simulation was controlled by a Nosé–Hoover chain thermostat.¹⁵ To study the temperature dependency of the sodium cluster polarizabilities the polarizability tensor was calculated along the recorded trajectories. For this purpose the first 20 ps of each trajectory were discarded and α was then calculated in 100 fs time steps along the remaining 200 ps. Due to the computational demand of the analytical polarizability calculation along the BOMD trajectories we employed the LDA kernel. Thus, the computational level for the calculation of the temperature-dependent part of the cluster polarizabilities is VWN/TZVP-FIP/GEN-A2*. The temperature-dependent mean sodium cluster polarizability is then calculated as:

$$\bar{\alpha}(T) = \bar{\alpha}^{\text{PBE}}(0) + \delta\bar{\alpha}^{\text{VWN}}(T) \quad (1)$$

with

$$\bar{\alpha}(T) = \frac{1}{3}[\bar{\alpha}_{xx}(T) + \bar{\alpha}_{yy}(T) + \bar{\alpha}_{zz}(T)] \quad (2)$$

This approximation assumes that the temperature dependency of $\alpha(T)$, namely $\delta\bar{\alpha}(T)$, is the same at PBE and VWN levels of theory. It should be remembered that the geometries are of course always resulting from PBE BOMD calculations. In Figure 1 the calculated cluster polarizabilities at 0 (a), 300 (b), 500 (c), and 700 K (d) are depicted. As this figure shows the individual cluster polarizabilities increase with temperature. Somewhere between 500 and 700 K the calculated $\bar{\alpha}(T)$ per atom match into the experimental data sets. In particular, the comparison of the calculated and experimental $\bar{\alpha}(T)$ per atom at 700 K for Na_7 , Na_8 , and Na_9 , for which excellent agreement between the different experimental data sets exist, is very satisfying. It is important to mention that the cluster temperature in experiment is estimated to be between 400 and 800 K. Moreover, it is interesting to note that the oscillating behavior of the $\bar{\alpha}$ per atom for the smaller clusters, which was observed in the original measurement^{5c} and also appears, less pronounced, in the $T = 0$ K PBE calculations (Figure 1a, stars), disappears at higher temperatures. Instead, the $\bar{\alpha}$ per atom decreases monotonically from Na_3 to Na_8 . Therefore, the finite temperature polarizabilities show no characteristic oscillations for open and closed shell systems. Instead, they only reflect the shell closing at the dimer and octamer consistent with the jellium model. Our BOMD calculations also show that cluster fragmentations are not important for the cluster polarizabilities. Such fragmentations occur in our simulations above 800 K. The change in the trend of the $\bar{\alpha}$ per atom for the small sodium clusters with increasing temperature is due to the different temperature dependencies of the individual cluster polarizabilities.

In Figure 2a the temperature dependencies of the individual cluster polarizabilities are presented. In this graph the behavior of Na_4 is particular. Over a large temperature range up to 600 K the $\delta\bar{\alpha}(T)$ value for this cluster changes almost ideally linear with the temperature. A closer analysis reveals that in this

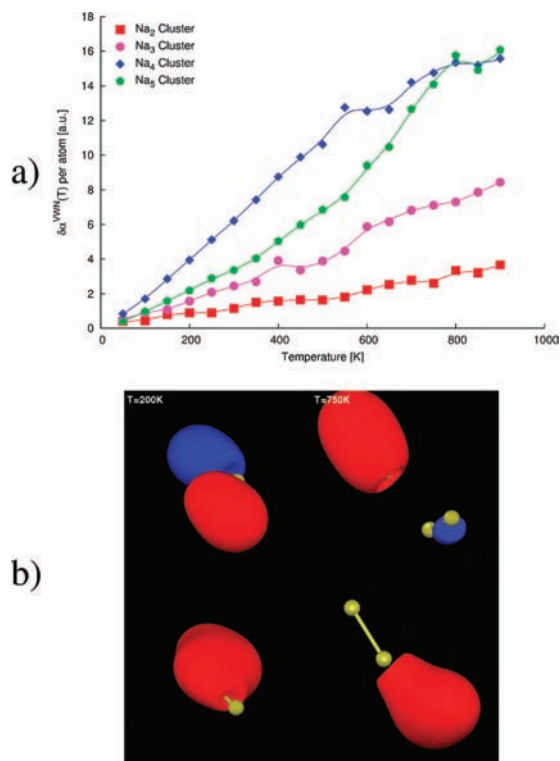


Figure 2. (a) Change of the mean polarizability per atom with temperature for Na_n clusters with $n = 2-5$. (b) The two highest occupied orbitals of Na_4 at 200 (left) and 750 K (right), respectively.

temperature range the D_{2h} rhombic structure of Na_4 rearranges only in the molecular plane. At 600 K and above three-dimensional rearrangements occur. In this case the temperature dependency of the polarizability reflects directly the dynamics of the cluster rearrangement. In Figure 2b typical snapshots of the highest occupied Na_4 molecular orbitals at 200 (left) and 750 K (right) during the cluster rearrangements are shown. At low temperature the s-type Na_4 orbital (nodeless) remains delocalized over the full system (lower orbital on the left side of Figure 2b), whereas at higher temperature this orbital correlates with the HOMO forming two Na_2 s-type orbitals. As a consequence the two Na_2 fragments can rearrange over three-dimensional transition states. Figure 2a also shows that $\delta\bar{\alpha}(T)$ increases considerably faster with temperature for Na_4 than for Na_5 . As a result, the bump in the static $T = 0$ K PBE polarizabilities at the pentamer (Figure 1a) disappears for the finite temperature polarizabilities.

In conclusion we have shown that the calculated $\bar{\alpha}(T)$ per atom match well with the available experimental data sets at around 700 K. Thus, the long-standing discrepancy between theory and experiment is resolved by inclusion of finite temperature effects in the electronic structure calculation. The calculated finite temperature sodium cluster polarizabilities show characteristic minima at the dimer and octamer as expected from the jellium model. However, individual molecular structures besides these two are not resolved in the calculated finite temperature sodium cluster polarizabilities.

Acknowledgment. This work is supported by the CONACyT projects 60117-U and 48775-U. G.U. Gamboa gratefully acknowledges a CONACyT Ph.D. fellowship (200113).

References and Notes

- (1) (a) Bonin, K. D.; Kresin, V. V. In *Electric-Dipole Polarizabilities of Atoms, Molecules and Clusters*; World Scientific: Singapore, 1997. (b) Knickelbein, M. B. *J. Chem. Phys.* **2004**, *120*, 10450–10454.
- (2) Pearson, R. G. *Science* **1966**, *151*, 172–177.
- (3) Knight, W. D.; Clemenger, K.; de Heer, W. A.; Saunderson, M. Y.; Chou, W. A.; Cohen, M. L. *Phys. Rev. Lett.* **1984**, *52*, 2141–2143.
- (4) Bergeron, D. E.; Roach, P. J.; Castleman, A. W., Jr.; Jones, N. O.; Khanna, S. N. *Science* **2005**, *307*, 231–235.
- (5) (a) Molof, R. W.; Miller, T. M.; Schwartz, H. L.; Benderson, B.; Park, J. T. *J. Chem. Phys.* **1974**, *61*, 1816–1822. (b) Knight, W. D.; Clemenger, K.; de Heer, W. A.; Saunders, W. A. *Phys. Rev. B* **1985**, *31*, 2539–2540. (c) Rayane, D.; Allouche, A. R.; Benichou, E.; Antoine, R.; Aubert-Frecon, M.; Dugourd, Ph.; Broyer, M.; Ristori, C.; Chandezon, C.; Hubert, B. A.; Guet, C. *Eur. Phys. J. D* **1999**, *9*, 243–248. (d) Tikhonov, G.; Kasperovich, V.; Wong, K.; Kresin, V. V. *Phys. Rev. A* **2001**, *64*, 063202–063205.
- (6) (a) Chandrakumar, K. R. S.; Ghanty, T. K.; Ghosh, S. K. *J. Chem. Phys.* **2004**, *120*, 6487–6494. (b) Kümel, S.; Akola, J.; Manninen, M. *Phys. Rev. Lett.* **2000**, *84*, 3827–3830. (c) Blundell, S. A.; Guet, C.; Zope, R. R. *Phys. Rev. Lett.* **2000**, *84*, 4826–4829. (d) Kronik, L.; Vasiliev, I.; Chelikowsky, J. R. *Phys. Rev. B* **2000**, *62*, 9992–9995.
- (7) (a) Hohenberg, P.; Kohn, W. *Phys. Rev.* **1964**, *136*, B864–866. (b) Kohn, W.; Sham, L. J. *Phys. Rev.* **1965**, *140*, A1133–1136.
- (8) Köster, A. M.; et al., deMon developers, 2006, <http://www.demon-software.com>.
- (9) Dirac, P. A. M. *Proc. Cambridge Philos. Soc.* **1930**, *26*, 376–385.
- (10) Vosko, S. H.; Wilk, L.; Nusair, M. *Can. J. Phys.* **1980**, *58*, 1200–1211.
- (11) Perdew, J. P.; Burke, K.; Ernzerhof, M. *Phys. Rev. Lett.* **1996**, *77*, 3865–3868.
- (12) Godbout, N.; Salahub, D. R.; Andzelm, J.; Wimmer, E. *Can. J. Phys.* **1992**, *70*, 560–571.
- (13) Calaminici, P.; Jug, K.; Köster, A. M. *J. Chem. Phys.* **1999**, *111*, 4613–4620.
- (14) Köster, A. M.; Reveles, J. U.; del Campo, J. M. *J. Chem. Phys.* **2004**, *121*, 3417–3424.
- (15) (a) Nosé, S. *J. Chem. Phys.* **1984**, *81*, 511–519. (b) Hoover, W. G. *Phys. Rev. A* **1985**, *31*, 1695–1697. (c) Martyna, G. J.; Klein, M. L.; Tuckerman, M. *J. Chem. Phys.* **1992**, *97*, 2635–2643.

JP808020F